Light Metals 2015
Edited by: Margaret Hyland
TMS (The Minerals, Metals & Materials Society), 2015

DETAILED MODEL OF ELECTROCHEMICAL CATHODE WEAR IN HALL-HÉROULT CELLS

Tao Li[1], Stein Tore Johansen[1, 2], and Asbjørn Solheim[2]

[1] Department of Energy and Process Engineering, Norwegian University of Science and Technology, Trondheim, Norway
[2] SINTEF Materials and Chemistry, Trondheim, Norway

Keywords: Cathode wear, electrochemical, aluminium carbide, bath film

Abstract

Clarification of the underlying chemistry and physics is critical for understanding the "double W" wear pattern of the carbon cathode observed in Hall-Héroult cells. Many studies have pointed out that aluminium carbide formation on the cathode surface is the dominating process that determines the cathode wear. However, the mechanisms of aluminium carbide formation on the carbon cathode surface are still not well clarified. In this study, previous work on cathode wear mechanism is summarized. The region between molten aluminium and the carbon cathode is considered as a small "local electrolysis cell" involving the aluminium pad, a bath film, an aluminium carbide layer, and the carbon cathode. The aluminium carbide formation rate is proportional to the current through the "local electrolysis cell" which is obtained by applying Ohm's law to the current and voltage of the electro-chemical reaction. A model is established for calculating the aluminium carbide formation rate as well as the cathode wear rate.

Introduction

The non-uniform wear of the cathode is presently one of the main limiting factors for the operational lifetime of aluminium reduction cells. The wear profile of cathode has been found to follow a "W" pattern, particularly in high amperage cells with highly conducting graphitized cathode blocks [1]. Recently, Skybakmoen *et al.* [2] reported a "double W" pattern in used cathodes by laser scanning measurements. The lifetime of the cathode depends on the zone with the heaviest wear.

Cathode wear has been attributed to physical abrasion and chemical corrosion [3]. However, the detailed cathode wear mechanisms are still on the way to be fully clarified. Liao and Øye [4] concluded that chemical corrosion is a stronger wear process than physical abrasion. Coupled diffusion experiments were carried out by Novak *et al.* [5, 6], which revealed that the existence of cryolite accelerates the chemical formation of aluminium carbide at the carbon-aluminium interface, and the thickness of the aluminium carbide layer is dependent on the local amount of cryolite. The presence of an electric field enhanced the formation rate of aluminium carbide. Furthermore, it was found that the aluminium carbide layer grows from the bottom of the layer [7]. Many researchers [4-13] have concluded that electrochemical formation of aluminium carbide is probably dominant in the cathode wear mechanism. However, the factors affecting the aluminium carbide formation rate on the cathode surface is still not well clarified.

In the present study, previous work on the cathode wear mechanism is summarized, and a model of cathode wear is established by dynamic calculation of aluminium carbide formation rate. The removal of aluminium carbide is qualitatively discussed as well.

Mechanism of Aluminium Carbide Formation

Aluminium Carbide Layer Covering the Cathode

Østrem *et al.* [3] studied cathodes from shut down of aluminium electrolysis cells. Aluminium carbide was found at the surface and in superficial pores of all the cathodes investigated. A continuous aluminium carbide layer with thickness of approximately 50 μm and up to more than 200 μm was observed on the cathode surface.

Sludge and Bath Film

Østrem [3] reported that there is bath between the carbon cathode and the metal pad; this was based on a large amount of samples. Apparently, bath penetrates the entire cathode and it can be found in most of the pores in the cathode. The bath appeared to have solidified as a continuous film at the cathode surface. The formation and refreshment of the bath film was related to formation and dissolution of sludge at the bottom of the cell. The sludge can be described as loosely packed alumina in which the voids are filled with bath, which contains in average about 40% Al_2O_3 [14]. The amounts and chemical composition of the sludge varies with the location. The NaF/AlF_3 molar ratio (CR) of the bath in the sludge is about 2.5 in samples taken below the feeding point, which is higher than in samples taken at the periphery of the cathode [15]. The fresh bath entrapped in the sludge may partly enter into the bath film between the aluminium pad and the aluminium carbide layer, which has a critical influence of the aluminium carbide removal rate as explained in the following section.

Electrochemical Formation of Aluminium Carbide

Cathode wear test experiments were performed by Tschöpe *et al.* ([12, 16] to evaluate and rank the performance of carbon cathode materials. It was found that the cathode wear rate increased significantly with increasing cathodic current density. Although the chemical formation of aluminium carbide is possible, electrochemical formation of aluminium carbide dominates in the cathode wear mechanism.

The concept of a "carbon pump" was proposed by Solheim and Tschöpe [13]. The concept involves a layer of aluminium carbide which contains pores filled with electrolyte. The latter is considered as a small electrolysis cell. Porous aluminium carbide is formed on the surface of the carbon cathode, while the aluminium carbide is oxidized at the top of the pore, and carbon enters into the molten aluminium. This forms a "pump" where carbon is transported from the carbon cathode and into the metal. The aluminium carbide formation rate could be derived from the voltage drop in the pore. However, the bath film between the aluminium carbide layer and aluminium pad was not considered in this mechanism. The carbon produced in the local anode reaction is not necessarily dissolved directly into the metal.

Detailed Electrochemical Wear Model

Aluminium Carbide Formation in "Local Electrolysis Cell"

It was assumed that a bath film fills the gap between the aluminium pad and the aluminium carbide layer covering the cathode carbon. Figure 1 illustrates the electrochemical reactions in the bath film and also shows the corresponding electric circuit. The cathode reaction at the bottom of the bath-filled pore is the same as that of the "carbon pump" model [13], while molten aluminium is involved in the anode reaction when the bath film is present. The current passes through the bath film and pores in the aluminium carbide layer from the anode to the cathode. The bath film is assumed to have uniform composition due to convection caused by the flow of molten aluminium.

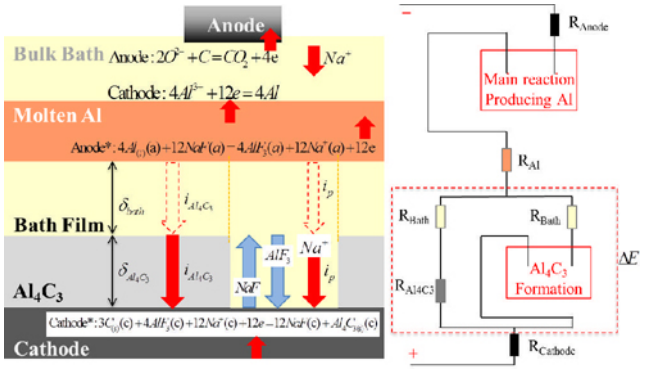

Figure 1. Electrochemical reactions in the bath film and pore, and the corresponding electric circuit.

The total local cell reaction becomes,

$$3C_{(s)}(c)+4AlF_3(c)+12Na^+(c)+4Al_{(l)}(a)+12NaF(a)= 4AlF_3(a)+12Na^+(a)+12NaF(c)+Al_4C_{3(s)}(c) \quad (1)$$

The activities of Na^+, Al_4C_3, and C are unity. Therefore, the reversible voltage is given by,

$$E^{rev}=E^0+\frac{RT}{12F}\ln\frac{a^4_{AlF_3(a)}a^{12}_{NaF(c)}}{a^4_{AlF_3(c)}a^{12}_{NaF(a)}} \quad (2)$$

where E^{rev} is the reversible voltage, E^0 is the standard cell voltage; R is the universal gas constant; T is the operating temperature; and F is Faraday's constant.

The standard voltage is derived from the chemical formation of Al_4C_3 by Al and C,

$$E^0=-\frac{\Delta G^0{}_{Al_4C_3}(T)}{12F}=-\frac{\Delta G^0{}_{Al_4C_3}(1233K)}{12F}=127mV \quad (3)$$

By considering the electric circuit shown in Figure 1, the voltage drop becomes,

$$i_{Al_4C_3}\left(\frac{\delta_{bath}}{\sigma_{bath}}+\frac{\delta_{Al_4C_3}}{\sigma_{Al_4C_3}}\right)=E^{rev}+i_p\left(\frac{\delta_{bath}+\delta_{Al_4C_3}\tau_b}{\sigma_{bath}}\right)=\Delta E \quad (4)$$

where ΔE is the voltage drop in the bath film and the pore in aluminium carbide layer; i is current density (through the pores and solid aluminium carbide layer respectively), δ is layer thickness, σ is electrical conductivity, and τ is the tortuosity of the pore.

The total current density though the Hall-Héroult cell is given by

$$i_{total}=i_{Al_4C_3}(1-\varphi)+i_p\varphi \quad (5)$$

With fixed ΔE, the current density through the pore can be obtained by solving Eqs. (2) and (4).

As in the "carbon pump" model [13], the transient wear rate at the bottom of the pore is given by Faraday's law,

$$\frac{dm_c}{dt}=-\frac{i_pM_c}{12F}n\frac{\pi}{4}d_p^2 \quad (6)$$

where M_c is the molar weight of carbon, n is the number density of pores [m^{-2}], and d_p is the pore diameter [m^{-2}]. The product of pore cross-sectional area and the number density of pores is the porosity (φ) which indicates the fraction of the aluminium carbide filled with bath. The average wear rate in terms of change in height becomes

$$\frac{dh_c}{dt}=-\frac{1}{\rho_c}\frac{dm_c}{dt}=-\frac{i_pM_c}{12F\rho_c}\varphi \quad (7)$$

where ρ_c is the density of aluminium carbide layer.

The transient growth rate of the aluminium carbide layer can now be calculated considering the influence of the porosity on its density,

$$\frac{dh_{Al_4C_3}}{dt}=\frac{1}{(1-\varphi)\rho_{Al_4C_3}}\frac{dm_{Al_4C_3}}{dt}=\frac{i_pM_{Al_4C_3}}{4F\rho_{Al_4C_3}}\frac{\varphi}{1-\varphi} \quad (8)$$

It is evident that the transient cathode wear rate and the aluminium carbide formation rate are proportional to the current density through the pores (i_p), which can be derived from Eqs. (4) and (5) when the reversible voltage across cell is known. The reversible voltage depends on the activities of AlF_3 and NaF; see Equation (2).

Ideal Temkin Activities

Many efforts have been made to clarify the structure of the NaF-AlF_3 system [16, 17]. The Temkin activity model is based on ionic fractions in an anionic lattice interwoven with a cation lattice. In an ideal Temkin model, the activity of each structural entity can be calculated, and the activities of NaF and AlF_3 become,

$$a_{NaF}=a_{Na^+}a_{F^-}=\frac{c_{Na^+}}{\sum c_+}\frac{c_{F^-}}{\sum c_-}=\frac{c_{F^-}}{\sum c_-}=x_{F^-} \quad (9)$$

$$a_{AlF_3}=\frac{a_{AlF_6^{3-}}}{a^3_{F^-}}=\frac{x_{AlF_6^{3-}}}{x^3_{F^-}} \quad (10)$$

where x denotes the molar fraction of ions and c denotes the molar concentration of ions. The activity of Na^+ is unity because it is assumed to be the only cation present.

By using Eqs. (9) and (10), Equation (2) can be rewritten,

$$E^{rev}=E^0+\frac{RT}{3F}\ln\left(\frac{x_{AlF_6^{3-}(a)}\cdot x^6_{F^-(c)}}{x_{AlF_6^{3-}(c)}\cdot x^6_{F^-(a)}}\right) \quad (11)$$

The transfer of NaF and AlF_3 in the bath film and pores shown in Figure 1 actually takes place by Na^+ migration and diffusion of anionic species. Following Solheim [17] we assume the anions to be F^-, AlF_6^{3-}, AlF_5^{2-}, AlF_4^-, and $Al_2F_7^-$ which are notified by successive numbers in the equations below. The molar concentration and fraction of these ions can be determined by three equilibria between the anions and the element balance of the NaF-AlF_3 system, as described in earlier work [17]. In the present study, rapid and precise solutions were obtained in MATLAB using the Newton iteration method.

Transport of Ions

The transfer of NaF and AlF_3 must be clarified in order to obtain their activities at the cathode (bottom of pore) and the anode (top of bath film). To fulfil the criterion of electro-neutrality at every point in the system, the ionic fluxes are represented as the motion of neutral substances, such as NaF, Na_3AlF_6, Na_2AlF_5, $NaAlF_4$, and $NaAl_2F_7$ (this is convenient since Na^+ is the only cation present). The same notations as in the Temkin activity model are used. Diffusion in a multi-component system can only be accurately described by the Stefan-Maxwell equations [17],

$$\nabla x_i = \sum_{j=1}^{n} \frac{1}{c_{tot} D_{ij}} (x_i J_j - x_j J_i) \tag{12}$$

where x_i is the molar fraction of component i, c_{tot} is the total molar concentration [mol·m^{-3}], D_{ij} (= D_{ji}) is the binary diffusion coefficient for the system i-j [m^{2}s^{-1}], and J is the molar flux [mol·m^{-2}s^{-1}].

The total concentration of the components is given by,

$$c_{tot} = \frac{\rho_{NaF-AlF_3}}{\sum_{i=1}^{n} x_i M_i} \tag{13}$$

where M_i is the molar weight of the neutral components and ρ is the density of the melt [19].

In the present study, the Stefan-Maxwell equations are applied to the system with five components, which gives five equations on the form,

$$\Delta x_1 = \frac{\Delta y}{\bar{c}_{tot}} \left(\frac{\bar{x}_1 J_2 - \bar{x}_2 J_1}{D_{12}} + \frac{\bar{x}_1 J_3 - \bar{x}_3 J_1}{D_{13}} + \frac{\bar{x}_1 J_4 - \bar{x}_4 J_1}{D_{14}} + \frac{\bar{x}_1 J_5 - \bar{x}_5 J_1}{D_{15}} \right) \tag{14}$$

where Δx_1 is the difference on molar fraction of component 1 between neighbouring elements (which is the activity difference, at distance Δy apart, which is the driving force for diffusion) and the over bars denotes average values of neighbouring elements.

Flux of the Components

Besides fulfilling the Stefan-Maxwell equations and the electro-neutrality criterion, all the ions should be at equilibrium based on the ideal Temkin model.

Although all the current is supposed to be carried by Na^+, aluminium is the only element that actually has a non-zero transport between the anode and the cathode. Thus, the flux of Al is given by,

$$J_{Al} = -\frac{i_p}{3F} \tag{15}$$

and the migration rate of Na^+ becomes,

$$J_{Na,Mig} = -\frac{i_p}{F} = 3J_{Al} \tag{16}$$

The fluxes of all the elements and components are given by,

$$J_F = J_1 + 6J_2 + 5J_3 + 4J_4 + 7J_5 = 0 \tag{17}$$

$$J_{Na} = J_1 + 3J_2 + 2J_3 + J_4 + J_5 + 3J_{Al} = 0 \tag{18}$$

$$J_{Al} = J_2 + J_3 + J_4 + 2J_5 = -\frac{i_p}{3F} \tag{19}$$

It is evident that the total molar fraction of the five components is unity,

$$x_1 + x_2 + x_3 + x_4 + x_5 = 1 \tag{20}$$

Solutions and Results of the Diffusion Model

Solutions of the above model were provided by systematically changing J_3, J_4, and J_5 until the equilibrium based on the Temkin model were achieved at every point [17, 18]. The calculation is acelerated by damped-Newton iteration using MATLAB programs, which made it possible to develop a dynamic model to calculate cathode wear rate.

Figure 2 shows the concentration gradients of components in the pores as functions of the distance from "local anode" (CR= 3.0, i_p = 8000A/m^2). The molar fraction of F^- becomes unity at around 400 μm from the "local anode," which indicates unit activity of NaF and zero activity of AlF_3. A diffusion length of 400 μm is therefore the upper theoretical limit at this current density. The thickness of the aluminium carbide layer was reported to be about 50 μm and up to more than 200 μm [3]. The thickness of the bath film was not reported.

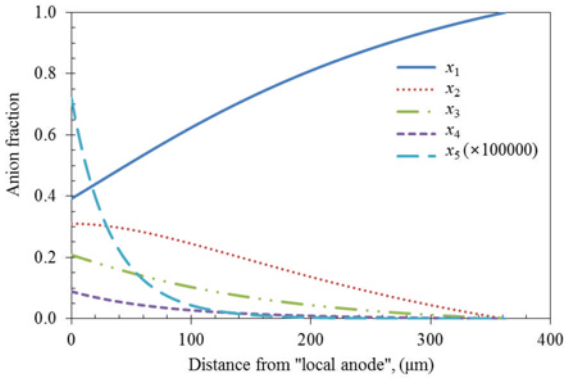

Figure 2. Concentration gradients as a function of distance from "local anode" (CR = 3.0, i_p = 8000A/m^2).

Figure 3 shows the reversible voltage with various CR at the top of the bath film ("local anode"). The current density is assumed to be 8000 A/m^2 inside the pores. The possible diffusion length increases somewhat with decreasing CR, but it is still limited to a short distance. When the thickness of the bath film is larger than the possible diffusion length, aluminium carbide cannot be formed. A way to lift this limitation is to assume that the diffusion barrier only takes place inside the pore, which means the CR in the bath film may be considered as a constant. This may indeed be the case in a non-stagnant bath film.

Figure 4 shows the reversible voltage as a function of the diffusion distance with various current densities through the pore.

As could be expected, the current density through the pores has a great influence on the reversible voltage. Still, the diffusion region is limited to some millimetres at i_p = 1000 A/m^2.

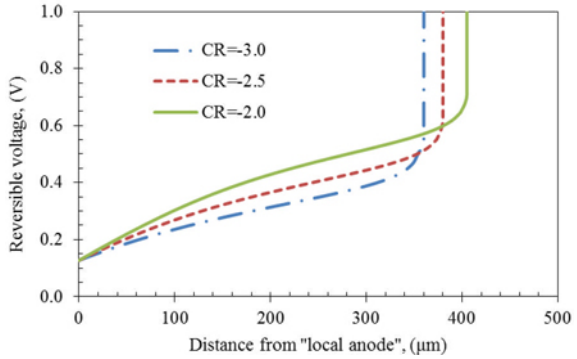

Figure 3. Reversible voltages with different CR at the "local anode" (i_p = 8000 A/m^2).

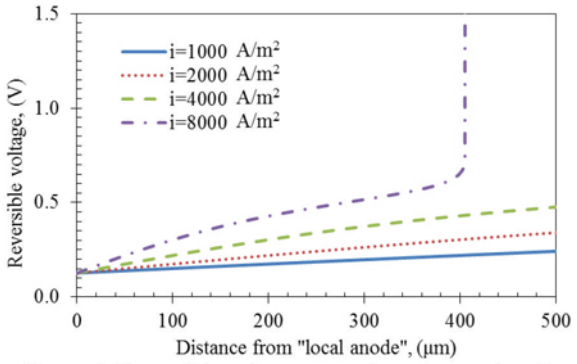

Figure 4. Reversible voltages at various current densities through pore (CR = 2.0).

Dynamic Model of Cathode Wear

Porosity and Tortuosity of the Aluminium Carbide Layer

Theoretically, the cathode wear rate can be calculated from Equation (7). However, the pore fraction and the tortuosity of pores for calculating the current density have not been investigated so far. The magnitude of these parameters can be approximately estimated by the operation parameters of a typical Hall-Heroult cell, assuming that the thickness of the bath film and the aluminium carbide layer are 1 mm and 10 μm, respectively; these numbers are somewhat arbitrary, but partly based on SEM images of bath film from Østrem [3]. The reversible voltage is assumed to be the minimum 0.127 V as the aluminium carbide layer is thin. The current density in the pores is set corresponding to the wear rate by Equation (7). The total current density is then obtained by Eqs. (4) and (5). Figure 5 and Figure 6 show the total current density through the cell as a function of the pore fraction calculated with different tortuosity. As can be observed, the tortuosity has little effect on the results of total current density. The general current density in the modern Hall-Héroult cells is around 8000 A/m^2. Therefore, the porosity of the aluminium carbide layer could be around 0.05. According to Figure 4, the reversible voltage increases slowly with increasing thickness of the aluminium carbide layer. Therefore, using the minimum reversible voltage is reasonable.

The tortuosity used in Figs. 5 and 6 was based on relationships suggested in the literature [20],

$$\tau_p = 1 - p\ln\varphi \quad \text{(p=0.5 for diffusion in a model of spheres)} \quad (21)$$

$$\tau_p = 1 + p\ln(1-\varphi) \quad \text{(p=2 for sand; p=3 for clay)} \quad (22)$$

$$\tau_p = \left[1 + p\ln(1-\varphi)\right]^2 \quad \text{(p=1.1 for diffusive in marine muds)} \quad (23)$$

Fixing the porosity at 0.05, the tortuosity calculated from the above equations is in the range 2.50-4.18 with average of 3.3 which is chosen for the calculation in this study.

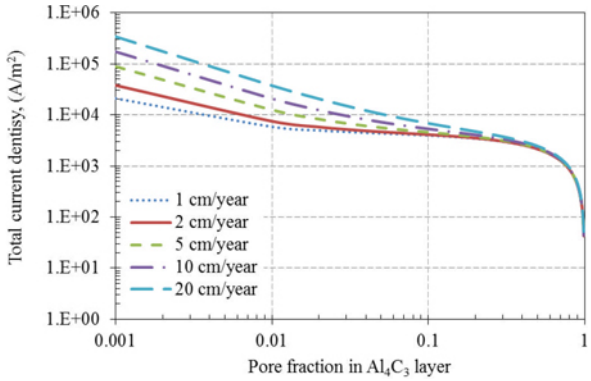

Figure 5. Total current density versus pore fraction (τ_p=1).

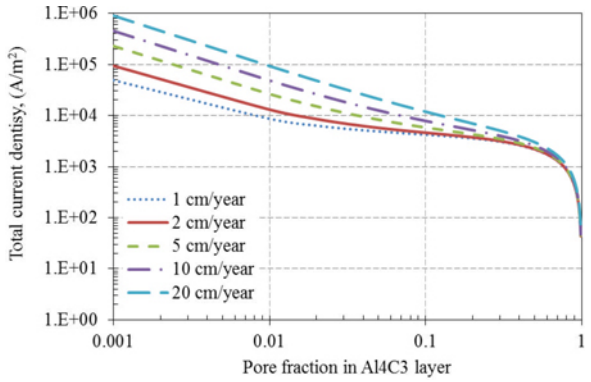

Figure 6. Total current density versus pore fraction (τ_p=3).

Aluminium Carbide Formation Rate

The voltage drop ΔE over the bath film and aluminium carbide layer cannot be directly measured in Hall-Héroult cells. Giving a reasonable assessment of the voltage drop is one of the ways to quantitatively investigate the cathode wear rate at this stage. NaF is found as a separate phase in the solidified bath inside the pores near the cathode surface, indicating that the local CR is greater than 3.0 [3]. It was thus proposed that the CR might be larger than 3.0 in the bath film which is very close to the cathode surface. However, the reason might also be that AlF_3 in the pores is consumed by the aluminium carbide formation. On the other hand, AlF_3 is produced in the half cell reaction at the top of the bath film, so the CR of the bath film may in fact be even smaller than the CR of the bulk of the bath. The CR was set as 2.0 in the calculations below.

Eqs. (7) and (8) give the transient aluminium carbide formation and cathode wear rate, which are proportional to the current density inside the pores. However, the reversible voltage increases with the growth of the aluminium carbide layer if its removal is

not considered. Therefore, the current density distribution between the solid aluminium carbide layer and the pores varies with time, even when the voltage drop is fixed. The thickness of the bath film is set at 1 mm.

Figure 7 a-c show the variation in aluminium carbide formation rate and thickness of the aluminium carbide layer with time at different voltage drops in the diffusion layer, while Figure 8 a-c shows the cathode wear rate and current density versus the thickness of the aluminium carbide layer. The aluminium carbide formation rate decreases with the growth of aluminium carbide layer which represents an increasing diffusion barrier. A very small current density in the pores would generate a quite high reversible voltage when the thickness of the aluminium carbide layer is thick. The aluminium carbide formation would stop without removal of aluminium carbide. The aluminium carbide formation rate goes higher along with larger ΔE. The aluminium carbide layer grows much thicker with higher ΔE without introducing the term of aluminium carbide removal. The thickness of aluminium carbide layer would be kept at a certain thickness, when the aluminium carbide removal rate reaches to the aluminium carbide formation rate at a local point. At the certain thickness of aluminium carbide layer, the cathode wear rate and total current density can be drawn from Figure 7 and Figure 8.

The normal total current density of the aluminium reduction cell is known to be around 8000 A/m^2. While ΔE = 0.15 V; according to Figure 8 (a), the thickness of the aluminium carbide layer may be kept at around 8 μm if the aluminium carbide removal rate could be around 7×10^{-9} m/s. The aluminium carbide layer is growing when the aluminium carbide removal rate is smaller than this; otherwise its thickness decreases.

The equilibrium thickness of aluminium carbide is probably between 12 μm and 25 μm; the aluminium carbide removal rate is correspondingly 3×10^{-8} m/s and 5×10^{-8} m/s from Figure 7. The local aluminium carbide layer plays a critical role on the current density distribution at the cell bottom.

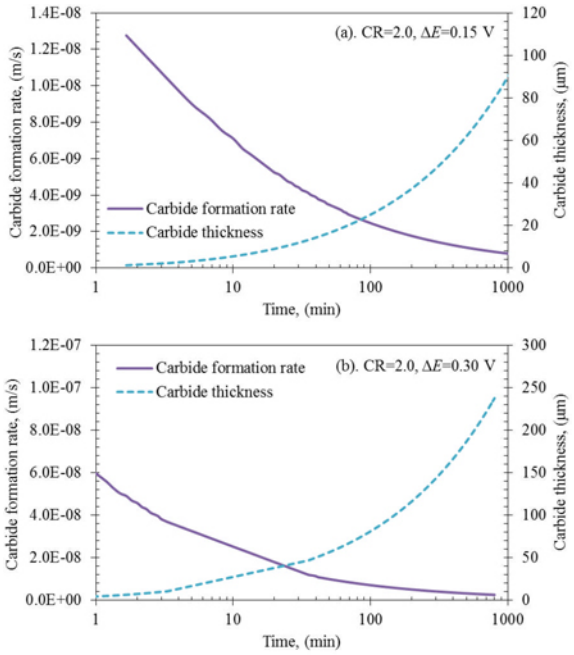

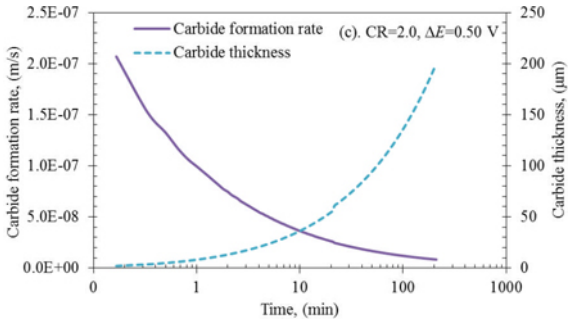

Figure 7. Change in aluminium carbide formation rate and thickness of carbide layer with time.

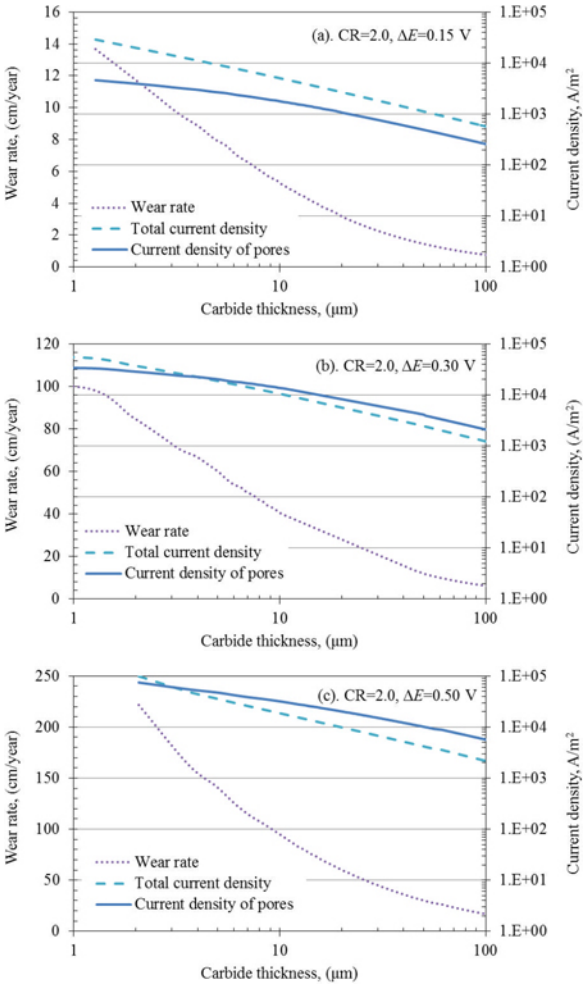

Figure 8. Cathode wear rate and current density versus thickness of aluminium carbide layer.

Removal of the Aluminium Carbide Layer

The aluminium carbide layer first dissolves into the bath film, and from there it is removed by refreshment of the film. To fully understand the removal rate of the dissolved aluminium carbide, it is necessary to resolve the mass distribution and the exchange rate of the sludge at the bottom of the cell. The distribution of sludge is influenced by the feeding process, chemical components in the

bath, and the flow pattern of molten aluminium. Local heat fluxes may also play a role. Local heating may partly come from the Joule heating of the aluminium carbide layer, since most current in the cell passes through the aluminium carbide layer other than the pores. Part of the dissolved aluminium carbide in the bath film will enter into the aluminium pad by diffusion, since aluminium has some carbon solubility. The details of the aluminium carbide layer removal will be investigated in future work.

Conclusions

Previous models for cathode wear are summarized. The electrochemical formation of aluminium carbide on the surface of the cathode carbon is supposed to be the key factor. The region between the aluminium pad and the cathode is considered to form a small local electrolysis cell, involving the aluminium pad, a bath film, an aluminium carbide layer with pores, and the surface of the cathode carbon. The aluminium pad and carbon cathode are the "local anode" and "local cathode" respectively.

1. The aluminium carbide formation rate and hence, the cathode wear rate, are proportional to the current density in pores distributed on the aluminium carbide layer.
2. A dynamic model for aluminium carbide formation and cathode wear is established without considering the details of aluminium carbide removal.
3. The porosity and tortuosity of the pores in the aluminium carbide layer was estimated from the average current density in Hall-Héroult cells. The porosity and tortuosity are supposed to be 0.05 and 3.3 respectively.
4. The growth of the aluminium carbide layer would stop at a certain thickness without introducing a special term describing aluminium carbide removal. The equilibrium thickness of the aluminium carbide layer was calculated as 8 μm, 12 μm and 25 μm at voltage drops of 0.15, 0.3, and 0.5 V. The aluminium carbide layer is growing when the local aluminium carbide removal rate is smaller than the formation rate; otherwise its thickness decreases. The thickness also acts as a critical factor on the current density distribution in the cell.

At present, experimental work for verifying the present model has not been planned, simply because it is very difficult to find good experimental methods in this field. Hopefully, ideas will emerge in the future.

Acknowledgement

The present work was carried out in the project Durable Materials in Primary Aluminium Production (DuraMat), financed by the research Council of Norway, Hydro Aluminium, Sør-Norge Aluminium (Søral), and Elkem Carbon. Permission to publish the results is gratefully acknowledged.

References

1. P. Reny and S. Wilkening, "Graphite Cathode Wear Study at Alouette," *Light Metals 2000*, 399-405.
2. E. Skybakmoen, S. Rørvik, A. Solheim, K.R. Holm, P. Tiefenbach, and Ø. Østrem, "Measurement of Cathode Surface Wear Profiles by Laser Scanning," *Light Metals 2011*, 1061-1066.
3. Ø. Østrem, "Cathode wear in Hall Héroult cells" (Ph.D. thesis, NTNU, 2012).
4. X. Liao and H. A. Øye, "Physical and chemical wear of carbon cathode materials," *Light Metals 1998*, 667-674.
5. B. Novak, K. Tschöpe, A. P. Ratvik, and T. Grande, "Fundamentals of aluminium carbide formation," Light Metals 2012, 1343-1348.
6. B. Novak, K. Tschöpe, A. P. Ratvik, and T. Grande, "The effect of cryolite on the formation of aluminium carbide at the carbon aluminium interface," *Light Metals 2012*, 1245-1250.
7. B. Novak, "On the chemical and electrochemical formation of aluminium carbide in aluminium electrolysis," (Ph.D. thesis, NTNU, 2013).
8. A. Zoukel, P. Chartrand, and G. Soucy, "Study of Aluminum Carbide Formation in Hall-Heroult Electrolytic Cells," *Light Metals 2009*, 1123-1128.
9. R. Keller, J. W. Burgman, and P. J. Sides, "Electrochemical Reactions in the Hall-Heroult Cathode," *Light Metals 1988*, 629-631.
10. X. Liao and H. A. Øye, "Carbon Cathode Corrosion by Aluminum Carbide Formation in Cryolitic Melts," *Light Metals 1999*, 621-627.
11. P. Rafiei, F. Hiltmann, M. Hyland, B. James, and B. Welch, "Electrolytic Degradation Within Cathode Materials," *Light Metals 2001*, 747-752.
12. K. Tschöpe, A. Støre, S. Rørvik, A. Solheim, E. Skybakmoen, T. Grande, and A. P. Ratvik, "Investigation of the Cathode Wear Mechanism in a Laboratory Test Cell," *Light Metals 2012*, 1349-1354.
13. A. Solheim and K. Tschöpe, "Model for Excessive Cathode Wear by a "Carbon Pump" at the Cell Bottom", *Light Metals 2013*, 1257-1262.
14. J. Thonstad, P. Johansen, and E. W. Kristensen, "Some Properties of Alumina Sludge," *Light Metals 1980*, 227-239.
15. F. Allard, M. A. Coulombe, G. Soucy, and L. Rivoaland, "Cartography and Chemical Composition of the Different Deposits in the Hall-Heroult Process," *Light Metals 2014*, 1233-1238.
16. K. Tschöpe A. Støre, E. Skybakmoen, A. Solheim, T. Grande, and A.P. Ratvik, "Critical Reflections on Laboratory Wear Tests for Ranking Commercial Cathode Materials in Aluminium Cells," *Light Metals 2013*, 1251-1256.
17. A. Solheim, "Concentration Gradients of Individual Anion Species in the Cathode Boundary Layer of Aluminium Reduction Cells," *Light Metals 2012*, pp. 665-470.
18. A. Solheim, "Some Aspects of Heat Transfer Between Bath and Sideledge in Aluminium Reduction Cells," *Light Metals 2011*, 381-386.
19. A. Solheim, "The Density of Molten NaF-LiF-AlF_3-CaF_2-Al_2O_3 in Aluminium Electrolysis," *Aluminium Transactions*, 2 (2000), 161-168.
20. M. Matyka, A. Khalili, and Z. Koza, "Tortuosity-porosity Relation in the Porous Media Flow," *Phys. Rev. E*, 78 (2008), 1-8.